


Article

Linear and Nonlinear Electrostatic Excitations and Their Stability in a Nonextensive Anisotropic Magnetoplasma

Muhammad Khalid ^{1,2}, Ata-ur-Rahman ¹, Ali Althobaiti ³ , Sayed K. Elagan ³, Sadah A. Alkhateeb ⁴, Ebtehal A. Elghmaz ⁵ and Samir A. El-Tantawy ^{6,7,*}

¹ Theoretical Plasma Physics Group, Islamia College Peshawar, Peshawar 25120, Pakistan; mkhalid_khan@yahoo.com (M.K.); ata@icp.edu.pk (A.-u.-R.)

² Department of Physics, Government Post Graduate College Mardan, Mardan 23200, Pakistan

³ Department of Mathematics, College of Science, Taif University, P.O. Box 11099, Taif 21944, Saudi Arabia; aa.althobaiti@tu.edu.sa (A.A.); skhalil@tu.edu.sa (S.K.E.)

⁴ Mathematics Department, Faculty of Science, University of Jeddah, Jeddah 23218, Saudi Arabia; salkhateeb@kau.edu.sa

⁵ Department of Physics, King Khalid University, P.O. Box 9004, Abha 61421, Saudi Arabia; egamaz@kku.edu.sa

⁶ Department of Physics, Faculty of Science, Port Said University, Port Said 42521, Egypt

⁷ Research Center for Physics (RCP), Department of Physics, Faculty of Science and Arts, Al-Baha University, Al-Baha 1988, Al-Mikhwah, Saudi Arabia

* Correspondence: tantawy@sci.psu.edu.eg



Citation: Khalid, M.; Ata-ur-Rahman; Althobaiti, A.; Elagan, S.K.; Alkhateeb, S.A.; Elghmaz, E.A.; El-Tantawy, S.A. Linear and Nonlinear Electrostatic Excitations and Their Stability in a Nonextensive Anisotropic Magnetoplasma. *Symmetry* **2021**, *13*, 2232. <https://doi.org/10.3390/sym13112232>

Academic Editor: Anton A. Kutsenko

Received: 23 October 2021

Accepted: 10 November 2021

Published: 22 November 2021

Publisher's Note: MDPI stays neutral with regard to jurisdictional claims in published maps and institutional affiliations.



Copyright: © 2021 by the authors. Licensee MDPI, Basel, Switzerland. This article is an open access article distributed under the terms and conditions of the Creative Commons Attribution (CC BY) license (<https://creativecommons.org/licenses/by/4.0/>).

Abstract: In the present work, the propagation of (non)linear electrostatic waves is reported in a normal (electron–ion) magnetoplasma. The inertialess electrons follow a non-extensive q -distribution, while the positive inertial ions are assumed to be warm mobile. In the linear regime, the dispersion relation for both the fast and slow modes is derived, whose properties are analyzed parametrically, focusing on the effect of nonextensive parameter, component of parallel anisotropic ion pressure, component of perpendicular anisotropic ion pressure, and magnetic field strength. The reductive perturbation technique is employed for reducing the fluid equation of the present plasma model to a Zakharov–Kuznetsov (ZK) equation. The parametric role of physical parameters on the characteristics of the symmetry planar structures such solitary waves is investigated. Furthermore, the stability of the pulse soliton solution of the ZK equation against the oblique perturbations is investigated. Furthermore, the dependence of the instability growth rate on the related physical parameters is examined. The present investigation could be useful in space and astrophysical plasma systems.

Keywords: anisotropic magnetoplasma; non-Maxwellian electrons; Zakharov–Kuznetsov solitons; oblique perturbations; stability analysis of ZK solitons

1. Introduction

Ion-acoustic waves (IAWs) play an essential part in studying the linear and nonlinear aspects among several astrophysical plasmas. Such types of wave modes are basically low-frequency longitudinal plasma density oscillations, which Tonks and Langmuir anticipated in 1929 [1], as they defined the phase velocity for isothermal changes and frequencies well below the ion plasma frequency. Moreover, in 1933, it was observed that the IAWs possess the electrical oscillations within an electrical discharge through gases by Revans [2].

A large number of researchers have studied the dynamics of the IAWs experimentally and theoretically in the last few decades [3–10]. There are many approaches for investigating the different types of nonlinear structures in plasma physics such as a reductive perturbation technique (RPT), Sagdeev potential approach, etc. For instance, Washimi and Taniuti [11], for the first time, used the RPT for studying the characteristics of the weakly nonlinear ion-acoustic solitons (IASs) in an electron–ion ($e-i$) plasma. On the other side, for investigating the arbitrary amplitude IAWs in the $e-i$ plasma, a fully nonlinear theory was reported by Sagdeev [12]. The planar solitary waves are characterized by a

high symmetry due to the balance between dispersion and nonlinearity. Ikezi et al. [13] experimentally proven the presence of ion-acoustic solitary waves (IASWs). The IASs with two different types of electrons (hot and cold) obeying non-extensive distribution have been studied by Saini and Shalini [14]. The presence of particles with nonextensive distribution shows that the characteristics of the IASs (compressive and rarefactive) in the given plasma system are drastically altered by changing the nonextensivity of electrons.

It is challenging to understand the nonextensive generalization of the Boltzmann–Gibbs–Shannon (BGS) entropy. This distribution is recognized for the first time by Renyi [15] and was later supported by Tsallis [16]. The well-known Maxwellian distribution in Boltzmann–Gibbs statistics is considered authentic universally for the macroscopic ergodic equilibrium systems. The Maxwellian distribution, however, may not be suitable for systems with long-range interactions and non-equilibrium static states, such as plasma and gravitational systems. The theory and experiment suggested that the BGS formalism is incapable of summarizing systems with long-range interactions and memory effects [16]. A number of irrefutable pieces of evidence indicate that the q -entropy may provide a valuable framework to analyze a range of astrophysical scenarios, including star polytropes, the solar neutrino challenge, and the unusual velocity distribution of galaxy clusters. The experimental results for electrostatic plane wave propagation in a collisionless thermal plasma led to a class of Tsallis' velocity distributions being characterized by a nonextensive q -parameter less than unity [17]. The term of matter nonextensivity has been effectively implemented in plasma physics [17–22]. In nonextensive plasmas, a group of communal phenomena like ion-acoustic (IA) waves, DIA waves, DA waves, and electron acoustic waves have been examined, be it by assuming electrons to be nonextensive [23] or ion nonextensive [24,25], or both electron and ion nonextensive. Cairns et al. [26] carried out a study on the effect of ion temperature, external static magnetic field, and oblique propagation on the structure of these solitary waves. Moreover, Mamun and Cairns considered the same problem for cold ions [27]. Therefore, they were able to show the existence of compressive and rarefactive solitary waves as well as the investigation of their stabilities. The Zakharov and Kuznetsov (ZK) equation was first derived using RPT to govern the IAWs in a magnetized plasma in 1974 [28]. Furthermore, Ladke and Spatschek [29], Infeld [30], and Das and Verheest [31] investigated the existence and stability of solitary waves in a plasma with external magnetic field [32]. The main objective of this paper is to investigate the impact of the non-Maxwellian (say nonextensive distributed) electrons on the characteristics of IASWs in a magnetized anisotropic plasma. To do that, the RPT could be employed for deriving the evolution equation, i.e., ZK equation is derived. Furthermore, the stability of the ZK solitary wave solution will be investigated.

2. The Physical Problem and Mathematical Model

We consider a collisionless magnetized plasma consisting of cold ions and nonextensive electrons. The plasma model is supposed to be in an external magnetic field $B = B_0 \hat{x}$ and the wave vector lie in the $x - y$ plane. The set of equations describing the IAWs in the present model may be explained by the mentioned sets of equations:

$$\partial_t n + \vec{\nabla} \cdot (n \vec{v}) = 0, \quad (1)$$

$$\partial_t \vec{v} + \vec{v} (\vec{\nabla} \cdot \vec{v}) = \frac{Ze}{m} \vec{E} + \frac{Ze}{mc} (\vec{v} \times B_0 \hat{x}) - \frac{1}{mn} \vec{\nabla} \cdot \tilde{P}, \quad (2)$$

and the pressure tensor \tilde{P} [33–36] is given as

$$\tilde{P} = p_{\perp} \hat{I} + (p_{\parallel} - p_{\perp}) \hat{b}, \quad (3)$$

here \hat{I} and \hat{b} represent, respectively, the unit tensor and unit vector along the external magnetic field. The parallel p_{\parallel} and perpendicular p_{\perp} components of the ion pressures are given by

$$\begin{cases} p_{\parallel} = p_{\parallel 0} \left(\frac{n}{n_0} \right)^3, \\ p_{\perp} = p_{\perp 0} \left(\frac{n}{n_0} \right), \end{cases} \quad (4)$$

where $p_{\parallel 0}$ and $p_{\perp 0}$ denote equilibrium values of the ion parallel and perpendicular pressure, respectively, and they are defined by

$$\begin{cases} p_{\parallel 0} = n_0 T_{\parallel}, \\ p_{\perp 0} = n_0 T_{\perp}. \end{cases} \quad (5)$$

It was assumed that the electron will obey the Tsallis distribution [37,38]

$$f_e(v_e) = C_q \left[1 - (q-1) \left(\frac{m_e v_e^2}{2T_e} - \frac{e\phi}{2T_e} \right) \right]^{1/(q-1)}. \quad (6)$$

Here, C_q indicates the constant of normalization it is given by

$$C_q = \begin{cases} n_{e0} \left(\frac{m_e}{2\pi k_B T_e} \right)^{\frac{1}{2}} \frac{\Gamma\left(\frac{1}{1-q}\right)(1-q)^{1/2}}{\Gamma\left(\frac{1}{1-q}-\frac{1}{2}\right)}, & \text{for } -1 < q \leq 1, \\ n_{e0} \left(\frac{m_e}{2\pi k_B T_e} \right)^{\frac{1}{2}} \frac{(q+1)}{2} \frac{\Gamma\left(\frac{1}{q-1}+\frac{1}{2}\right)(q-1)^{1/2}}{\Gamma\left(\frac{1}{q-1}\right)}, & \text{for } q \geq 1. \end{cases} \quad (7)$$

Integrating in the entire velocities, we get the normalized form of electron number density as [39–41]

$$n_e = [1 + (q-1)\phi]^{(q+1)/2(q-1)}. \quad (8)$$

The energy of the nonextensive electrons can be obtained as

$$E = \frac{1}{2} m_e \langle v_e^2 \rangle = \frac{\int \int \int v_e^2 f_e(v_e) d^3v}{\int \int \int f_e(v_e) d^3v} = \frac{T_e}{3q-1}. \quad (9)$$

As the energy is always positive, this is possible only for $q > \frac{1}{3}$ [38].

Equation (8) can be expanded in the power of potential as

$$n_e = 1 + \mu_1 \phi + \mu_2 \phi^2 + \dots, \quad (10)$$

where μ_1 and μ_2 are, respectively, defined as

$$\begin{cases} \mu_1 = \frac{1}{2}(1+q), \\ \mu_2 = \frac{(q+1)(3-q)}{8}. \end{cases} \quad (11)$$

The Poisson's equation for the given system is defined as

$$\nabla^2 \phi = n_e - n. \quad (12)$$

Consider the two-dimensional perturbations in the $x-y$ plane. As a result, the set of equations characterizing ion dynamics in the current model goes as follows:

$$\partial_t n + \partial_x(nv_x) + \partial_y(nv_y) = 0, \quad (13)$$

$$\partial_t v_x + (v_x \partial_x + v_y \partial_y) v_x = -\frac{\partial \phi}{\partial x} - p_1 n \partial_x n, \quad (14)$$

$$\partial_t v_y + (v_x \partial_x + v_y \partial_y) v_y = -\frac{\partial \phi}{\partial y} + \Omega v_z - \frac{p_2}{n} \partial_y n, \quad (15)$$

$$\partial_t v_z + (v_x \partial_x + v_y \partial_y) v_z = -\Omega v_y, \quad (16)$$

The Poisson's equation in normalized form is

$$\partial_x^2 \phi + \partial_y^2 \phi = n_e - n. \quad (17)$$

In the mentioned sets of above equations, m , e , n_e , n_{e0} , n , and n_0 represent the mass of ions, electron charge, electron density, electron equilibrium density, ion density, and ion equilibrium density, respectively. v_x , v_y , and v_z are the ion fluid velocity along the corresponding axis, respectively. The parameter $\Omega_i = \frac{eB_0}{mc}$ denotes the ion gyro-frequency, and the dimensionless parameter is defined as $\Omega = \Omega_i / (\omega_{pi})$.

All quantities in Equations (13)–(17) are scaled as follows: the number density (n) is scaled by its equilibrium value n_0 , the ion fluid velocity (v) is scaled by ion-acoustic speed $C_s = \sqrt{\frac{T_e}{m}}$, and the electrostatic wave potential ϕ is scaled the thermal potential e/T_e . The space and time variables are, respectively, scaled by Debye length $\lambda_D = \sqrt{\frac{T_e}{4\pi n_0 e^2}}$ and inverse plasma frequency $\omega_{pi}^{-1} = \sqrt{m/(4\pi n_0 e^2)}$. The quantity $p_1 = \frac{3p_{\parallel 0}}{n_0 T_e}$ indicates the normalized ion parallel pressure and $p_2 = \frac{p_{\perp 0}}{n_0 T_e}$ is the normalized ion perpendicular pressure, respectively.

3. Linear Analysis

By linearizing Equations (13)–(17) and adopting a standard way where the first-order perturbed quantities are related to $\exp i(k \cdot r - \omega t)$, the following linear dispersion was obtained:

$$\omega^4 - \omega^2 \left(\frac{k^2}{k^2 + \mu_1} + p_1 k_x^2 + p_2 k_y^2 + \Omega^2 \right) + \Omega^2 \left(\frac{k_x^2}{k^2 + \mu_1} + p_1 k_x^2 \right) = 0, \quad (18)$$

where k is the wave vector defined as $k^2 = k_x^2 + k_y^2$. Equation (18) is quadratic in ω^2 with their two possible roots:

$$\omega_{\pm}^2 = \frac{1}{2} \left[\frac{\left(\frac{k^2}{k^2 + \mu_1} + p_1 k_x^2 + p_2 k_y^2 + \Omega^2 \right) \pm \sqrt{\left(\frac{k^2}{k^2 + \mu_1} + p_1 k_x^2 + p_2 k_y^2 + \Omega^2 \right)^2 - 4\Omega^2 \left(\frac{k_x^2}{k^2 + \mu_1} + p_1 k_x^2 \right)}}{\right], \quad (19)$$

where ω_{\pm} give the fast and slow modes of the electrostatic waves. It is shown that the value of ω_{\pm} depends upon on non-extensivity of electrons q through μ_1 . Note that ω_- defines an acoustic mode and for a small value of k_x , we obtain

$$\lim_{k_x \rightarrow 0} \left(\frac{\omega_-}{k_x} \right) = \sqrt{\frac{1}{\mu_1} + p_1}. \quad (20)$$

Remembering that relation (20) represents the speed of sound for quasi-parallel propagation within the Tsallis distribution, there exists a similar relation (32) in the nonlinear analysis section below. In the same way, when $k \rightarrow 0$ and $p_1 \rightarrow 0$, then the fast mode of electrostatic waves reduces to $\omega_+ \rightarrow \Omega$.

3.1. Asymptotic Behavior

In order to summarize the ω_{\pm}^2 for small wave number values ($k_x \ll 1$ & $k_y \ll 1$), let us expand Equation (19) using Taylor expansion, one can obtain the expressions for ω_-^2 and ω_+^2 , respectively, in the following form:

$$\omega_-^2 \approx \left(\frac{1}{\mu_1} + p_1 \right) k_x^2 - \frac{1}{\mu_1^2} \left(\frac{1 + \mu_1(p_1 + p_2 + \mu_1 p_1 p_2)}{\Omega^2} + 1 \right) k_x^2 k_y^2 + O(k_x^3, k_y^3), \quad (21)$$

and

$$\omega_+^2 \approx \Omega^2 + \left(\frac{1}{\mu_1} + p_1 \right) k_y^2 + \frac{1}{\mu_1^2} \left(\frac{1 + \mu_1(p_1 + p_2 + \mu_1 p_1 p_2)}{\Omega^2} - 1 \right) k_x^2 k_y^2 + O(k_x^3, k_y^3). \quad (22)$$

3.2. Parametric Study of Dispersion Relation

It is seen from Equation (19) that the dispersion relation is a function of the parallel component of anisotropic ion pressure p_1 , component of perpendicular anisotropic ion pressure p_2 , non-extensivity of electrons q , and the magnetic field strength Ω . Therefore, it is important to study the impact of these parameters on the linear properties of the IAWs. The behavior of fast and slow modes versus parallel wave number k_x is depicted in Figure 1a–d for different physical parameters. Figure 1a shows that the frequency of both slow and fast electrostatic modes decreases with the enhancement of the electron nonextensivity parameter q . Note that q is more effective in the faster mode than the slower mode. The effect of the parallel component of anisotropic ion pressure, p_1 , is depicted in Figure 1b, which depicts that the phase velocity of both fast and slow modes of the IAWs increases with increasing p_1 . The effect of perpendicular component of anisotropic ion pressure p_2 is shown in Figure 1c). It observed that p_2 increase the upper mode of frequency, while the reverse effect is seen in the lower branch. The influence of magnetic field Ω on the phase speed is investigated in Figure 1d. One can see that for lower values of k_x , growing the magnetic field Ω leads to increase the phase speed related to fast modes, and attains a constant asymptotic value for higher values of k_x . Moreover, it is observed that the frequency gap within the faster and slower ion-acoustic modes decreases with increasing the Ω at large k_x . Similarly, for small values of k_x , it increases with magnetic field strength Ω .

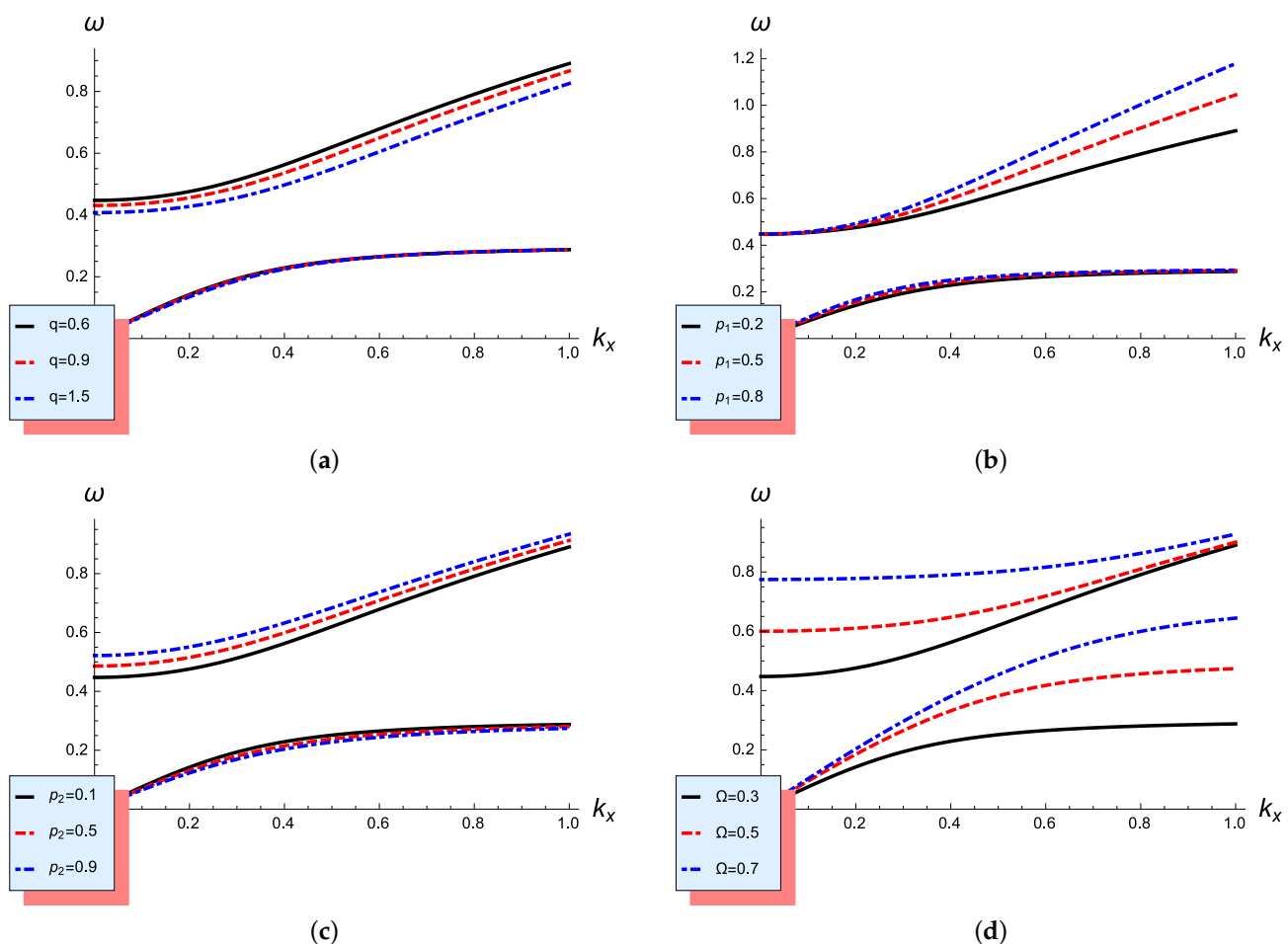


Figure 1. Graph of ω against k_x for (a) different q and fixed $p_1 = 0.2$, $p_2 = 0.1$, $\Omega = 0.3$; (b) different p_1 and fixed $q = 0.6$, $p_2 = 0.1$, $\Omega = 0.3$; (c) different p_2 and fixed $q = 0.6$, $p_1 = 0.2$, $\Omega = 0.3$; and (d) different Ω and fixed $q = 0.6$, $p_1 = 0.2$, and $p_2 = 0.1$.

3.3. Limiting Cases

We may consider some special cases, in which our algebraic analysis reduces to some special cases in the appropriate limit:

- (I) The cold electron ion model is recovered by setting $p_1 = p_2 = 0$.
- (II) When the nonextensivity parameter is $q \rightarrow 1$, then the Tsallis distribution adopted to Maxwell distribution.

3.3.1. Parallel Propagation

Consider the case of parallel propagation in which $k = k_x$ and $k_y = 0$, then Equation (18) can be reduced to the following form:

$$\omega_{\parallel}^2 = \frac{k^2}{k^2 + \mu_1} + p_1 k^2. \quad (23)$$

Relation (23) represents the dispersion relation of the electrostatic waves of magnetized plasma, with a parallel component of anisotropic ion pressure p_1 and Tsallis distributed electrons in case of parallel propagation. It is clear from relation (23) that ω_{\parallel}^2 does not depend on magnetic field.

3.3.2. Perpendicular Propagation

In this case, we consider $k_x = 0$ and $k = k_y$ which Equation (18) could be reduced to

$$\omega_{\perp}^2 = \frac{k^2}{k^2 + \mu_1} + \Omega^2 + p_2 k^2. \quad (24)$$

Here, relation (24) denotes the dispersion relation for electrostatic waves in a magneto-plasma, with Tsallis-distributed electrons and a component of perpendicular anisotropic ion pressure p_2 in the case of perpendicular propagation. It is clear from relation (24) that ω_{\perp}^2 is a function of magnetic field strength Ω and nonextensivity of electrons q through μ_1 and perpendicular component of anisotropic ion pressure p_2 .

4. Nonlinear Analysis and Derivation of ZK Equation

To study the small amplitude IAWs in the present model, the reductive perturbation method is introduced. Accordingly, the following new coordinates related to the none-static frame are introduced:

$$\begin{cases} X = \epsilon^{1/2}(x - \lambda t), \\ Y = \epsilon^{1/2}y, \\ \tau = \epsilon^{3/2}t, \end{cases} \quad (25)$$

where λ represents the phase velocity of the wave. The field dependent quantities are mentioned as

$$\begin{cases} n = 1 + \epsilon n_1 + \epsilon^2 n_2 + \epsilon^3 n_3 + \dots, \\ \phi = \epsilon \phi_1 + \epsilon^2 \phi_2 + \epsilon^3 \phi_3 + \dots, \\ v_x = \epsilon v_{x1} + \epsilon^2 v_{x2} + \epsilon^3 v_{x3} + \dots, \\ v_y = \epsilon^{3/2} v_{y1} + \epsilon^2 v_{y2} + \epsilon^{5/2} v_{y3} + \dots, \\ v_z = \epsilon^{3/2} v_{z1} + \epsilon^2 v_{z2} + \epsilon^{5/2} v_{z3} + \dots. \end{cases} \quad (26)$$

Substituting expansion (26) in Equations (13)–(17) and using Equation (25), we get the sets of expression in the order of expansion of $O(\epsilon^{\frac{3}{2}})$, in the simplified form as following

$$n_1 = \frac{v_{x1}}{\lambda} = \frac{1}{\lambda^2 - p_1} \phi_1, \quad (27)$$

$$v_{x1} = \frac{\phi_1}{\lambda} + \frac{p_1}{\lambda} n_1, \quad (28)$$

$$v_{y1} = 0, \quad (29)$$

$$\Omega v_{z1} = \partial_Y \phi_1 + p_2 \partial_Y n_1, \quad (30)$$

and in the Poisson's equation, the expansion order of $O(\epsilon^1)$ reads

$$n_1 = \mu_1 \phi_1. \quad (31)$$

Comparing Equations (27) and (31), we obtain the expression for phase velocity as follows:

$$\lambda = \sqrt{\frac{1}{\mu_1} + p_1}. \quad (32)$$

The phase velocity λ is plotted against the nonextensive parameter q for different values of parallel component of anisotropic ion pressure p_1 as shown in Figure 2. One can see from Figure 2 that the lower values of nonextensive parameter q correspond to higher phase velocity, and phase velocity decreases when q is increased. Furthermore, the phase velocity becomes constant when q approaches to 1. Moreover, we observe from Figure 2 that the phase velocity increases with increasing the parallel anisotropic ion pressure p_1 .

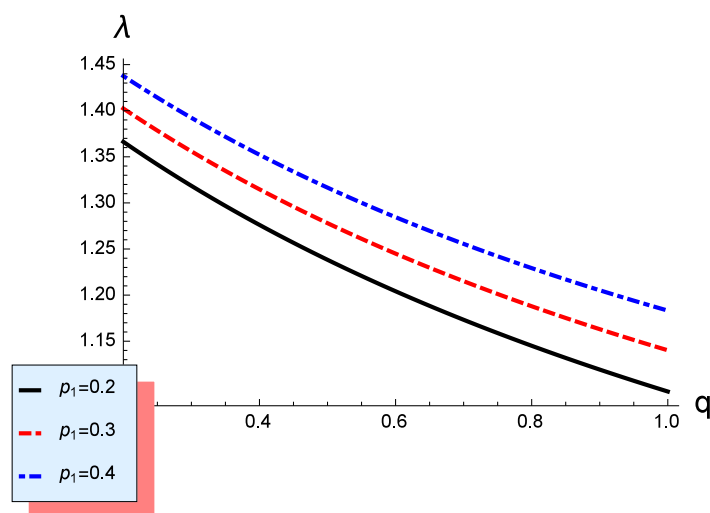


Figure 2. Graph of λ versus q for different values of p_1 .

Substituting expansion (26) in Equations (13)–(17) and using Equation (25), which for higher-order in ϵ , we get

$$\partial_\tau n_1 - \lambda \partial_X n_2 + \partial_X (n_1 v_{x1}) + \partial_X v_{x2} + \partial_Y v_{y2} = 0, \quad (33)$$

$$\partial_\tau v_{x1} - \lambda \partial_X v_{x2} + v_{x1} \partial_X v_{x1} + \partial_X \phi_2 + p_1 n_1 \partial_X n_1 + p_1 \partial_X n_2 = 0, \quad (34)$$

$$\Omega v_{z2} + \lambda v_{y1} = 0, \quad (35)$$

$$\lambda \partial_X v_{z1} - \Omega v_{y2} = 0, \quad (36)$$

and

$$n_2 = \mu_1 \phi_2 + \mu_2 \phi_1^2 - \partial_X^2 \phi_1 - \partial_Y^2 \phi_1. \quad (37)$$

Multiplying Equation (33) by λ and then adding to Equation (34), we get

$$\lambda \partial_\tau n_1 - (\lambda^2 - p_1) \partial_X n_2 + \lambda \partial_X (n_1 v_{x1}) + \lambda \partial_Y v_{y2} + \partial_\tau v_{x1} + v_{x1} \partial_X v_{x1} = -\partial_X \phi_2 - p_1 n_1 \partial_X n_1. \quad (38)$$

Making the use of Equations (27)–(37) in Equation (38), finally the following ZK equation is obtained ($\phi \equiv \phi_1$):

$$\partial_\tau \phi + A \phi \partial_X \phi + \partial_X (B \partial_X^2 \phi + C \partial_Y^2 \phi) = 0, \quad (39)$$

with

$$A = \frac{3\lambda^2 \mu_1^2 + p_1 \mu_1^2 - 2 \frac{\mu_2}{\mu_1}}{2\mu_1 \lambda}, \quad (40)$$

$$B = \frac{1}{2\mu_1^2 \lambda}, \text{ and } C = \frac{\Omega^2 + \lambda^2 \mu_1 (1 + p_2)}{2\lambda \mu_1^2 \Omega^2}. \quad (41)$$

5. Analytical Soliton Solution of the ZK Equation

The soliton solution of the ZK Equation (39) is defined by

$$\phi(\xi) = \phi_m \sec h^2 \left(\frac{\xi}{w} \right), \quad (42)$$

where $\xi = \chi(l_x X + l_y Y - u\tau)$ is the transformed coordinate and u is the speed of the nonlinear structure, and χ represents the inverse of soliton width. For wave vector k , the direction cosines are defined as l_x and l_y , respectively. $\phi_m = 3u/(l_x A)$ and $w = \sqrt{4(l_x^3 B + l_x l_y^2 C)}/u$ express the amplitude and width of the IASWs, respectively. The nonlinear coefficient A is sometimes positive and sometimes negative, while the dispersion coefficients B and C are always positive. Both polarity compressive and rarefactive nonlinear solitary waves are observed in the present plasma system. The amplitude of the solitary wave ϕ_m is depends on nonlinearity coefficient A and width of the solitary wave w are the functions of dispersion coefficients C and B .

6. Parametric Study

In this section, the effects of the physical parameters on the nonlinearity coefficient A and the dispersion coefficients B and C , will be investigated. In Figure 3, the nonlinearity coefficient A and the dispersion coefficients B and C are plotted versus the nonextensive parameter q and for different values of anisotropic ion pressure p_1 . It is seen that the nonlinearity coefficient A increases while dispersion coefficients B and C decrease with increasing q . Furthermore, we note that increases the value of anisotropic ion pressure p_1 leads to the enhancement of the nonlinearity coefficient A and dispersion coefficients C while reducing the dispersion coefficients B . It is important to mention here that the nonlinearity coefficient A is positive as shown from Figure 3. Therefore, in the present plasma system, only compressive solitary structures are observed.

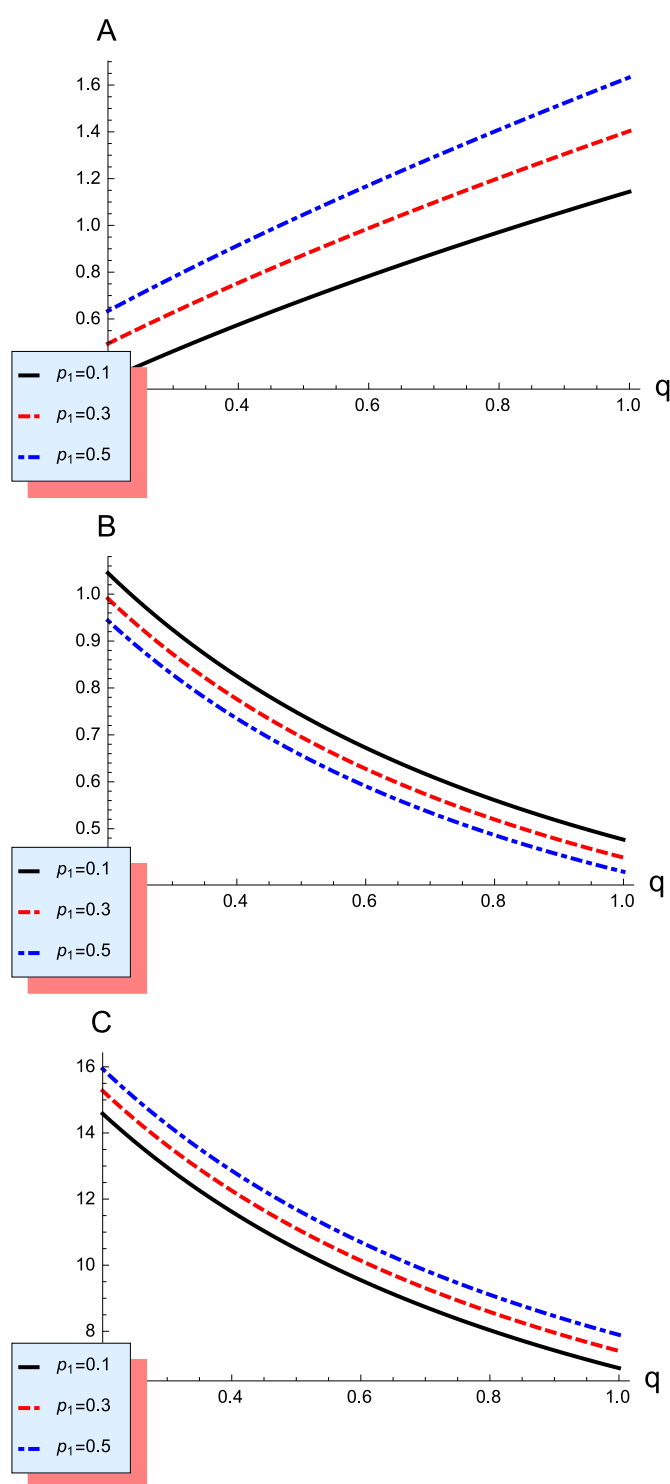


Figure 3. The coefficients A , B , C versus q for different values of p_1 and $\Omega = 0.3$.

It is clear from Equations (40) and (41) that the nonlinearity coefficient A and dispersion coefficient B are not based on Ω , while the dispersion coefficient C is based on the magnetic field strength Ω . However, it is essential to examine how Ω affects C . Figure 4 depicts how Ω affects C . Figure 4a is plotted for ($\Omega < 1$), while for the ($\Omega \geq 1$), Figure 4b is plotted. It should be observed that the C behaves identically in both circumstances, with the only difference being that the magnitude of C reduces in the presence of Ω .

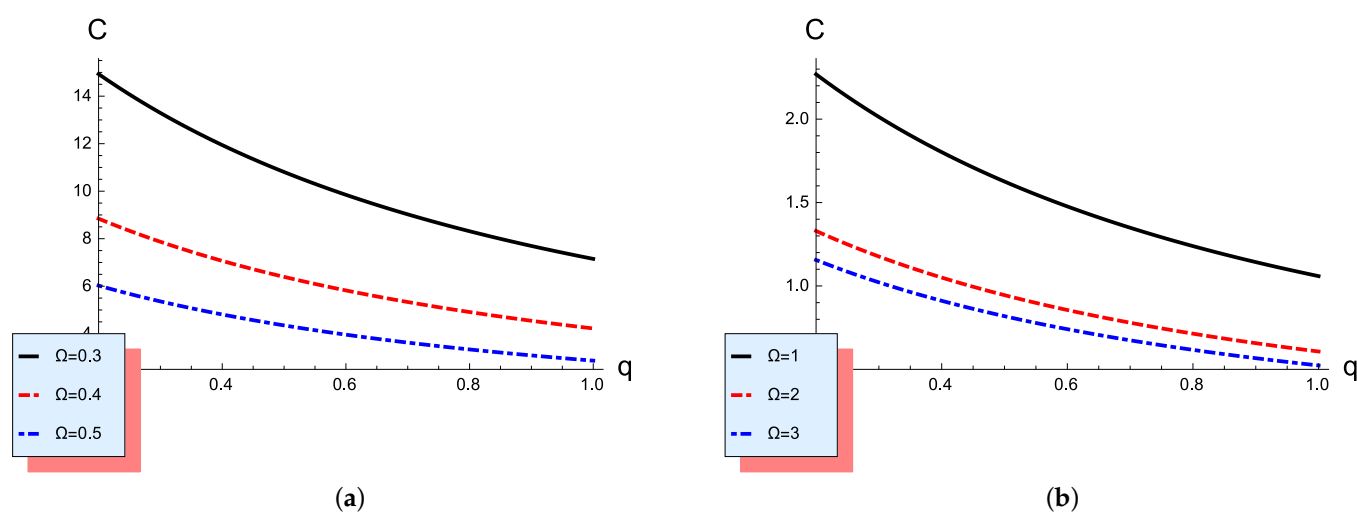


Figure 4. Coefficient C versus q (a) for $\Omega < 1$ and (b) for $\Omega > 1$ with fixed values of $p_1 = 0.2$ and $p_2 = 0.1$.

Figure 5 displays the effects of varies relevant parameters, namely, the nonextensivity parameter q , component of parallel anisotropic ion pressure p_1 , component of perpendicular anisotropic ion pressure p_2 , and the magnetic field strength Ω on the solitary wave profile. It is seen from Figure 5a that the amplitude and width of the IASWs increases with decreasing the nonextensive parameter q . In Figure 5b, the effect of p_1 on ion-acoustic nonlinear solitary wave potential $\phi(\xi)$ is investigated. Note from Figure 5b that higher p_1 minimizes the amplitude of positive potential IASWs. In Figure 5c, we investigate the impact of the directional cosine l_x on the solitary waves profile $\phi(\xi)$. This figure indicates that both the amplitude and width of compressive solitons decrease with increasing l_x . The effect of p_2 on the solitary waves profile $\phi(\xi)$ is investigated as shown in Figure 5d. It is observed that the width increases with increasing p_2 , while the amplitude remains unchanged. To demonstrate the effect of Ω on the ion-acoustic nonlinear solitary waves, Figure 5e is presented. It is found that the width of the IASWs decreases with increasing Ω , while the amplitude remains unchanged as shown in Figure 5e.

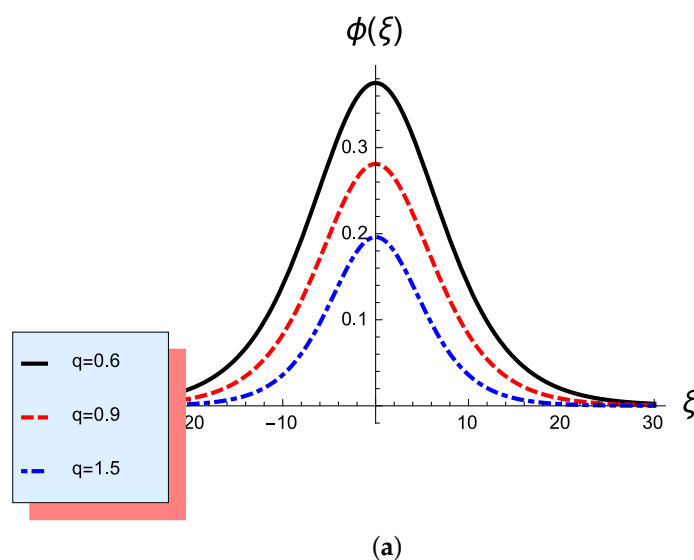


Figure 5. Cont.

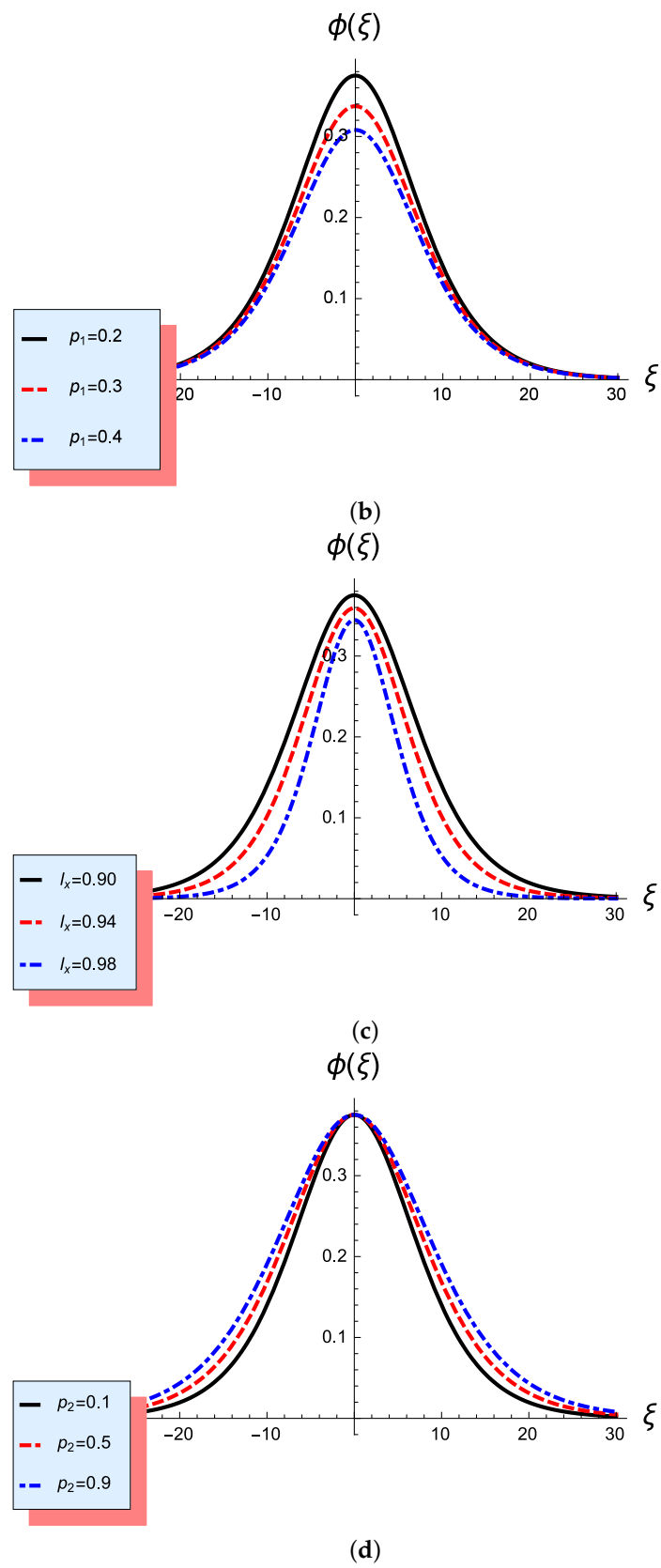


Figure 5. Cont.

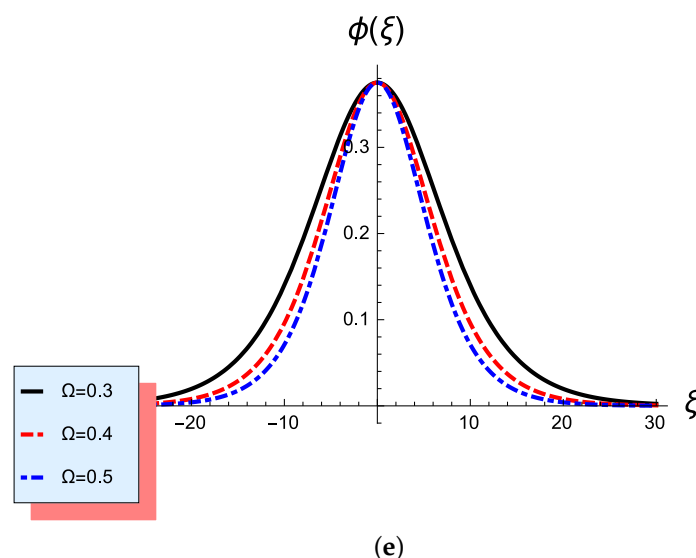


Figure 5. (a) Graph of solitary wave solution $\phi(\xi)$ versus ξ for different values of q , and $p_1 = 0.2$, $p_2 = 0.1$, $u = 0.1$, $\Omega = 0.3$, and $l_x = 0.9$. (b) Graph of solitary wave solution $\phi(\xi)$ versus ξ for different values of p_1 , and $q = 0.6$, $p_2 = 0.1$, $u = 0.1$, $\Omega = 0.3$, and $l_x = 0.9$. (c) Graph of solitary wave solution $\phi(\xi)$ versus ξ for different values of l_x and $p_1 = 0.2$, $p_2 = 0.1$, $u = 0.1$, $\Omega = 0.3$, and $q = 0.6$. (d) Graph of solitary wave solution $\phi(\xi)$ versus ξ for different values of p_2 , and $p_1 = 0.2$, $l_x = 0.9$, $u = 0.1$, $\Omega = 0.3$, and $q = 0.6$. (e) Graph of solitary wave solution $\phi(\xi)$ versus ξ for different values of Ω and $p_1 = 0.2$, $p_2 = 0.1$, $u = 0.1$, $l_x = 0.9$, and $q = 0.6$.

7. Pulse Stability Analysis

In order to analyze the stability of the soliton pulse solution (42), we will follow the same technique mentioned by Allen and Rowlands (AR) [42]. First, a transformation can be introduced in order to transform the planar ZK Equation (39) to its “canonical” form (cf. Equation (1.1) in [42]). Applying the transformation (see Appendix A in [43]), the planar ZK Equation (39) reduces to

$$\partial_{T'} \hat{\phi} + \hat{\phi} \partial_{X'} \hat{\phi} + \partial_{X'} \left[\partial_{X'}^2 \hat{\phi} + \partial_{Y'^2}^2 \hat{\phi} \right] = 0, \quad (43)$$

this equation is similar to Equation (1.1) in Ref. [42], (just $\hat{\phi}$ instead of n).

We concentrate on the major characteristics of Allen and Rowlands’ stability analysis [42] rather their derivations. The detail computation are mentioned in [42]. By following Allen and Rowlands [42], the solution of Equation (43) is assumed to be

$$\hat{\phi} = \phi_0 + \varepsilon \phi(x) \exp(\imath ky) \exp(\gamma t). \quad (44)$$

where ϕ_0 represents the exact solution of Equation (43), γ measures the instability growth rate, and k represents the wave vector transverse component. The quantity $\phi(x)$ can be determined later by using the multi-scale perturbation technique, relying on an expansion in k (for more details see in [42]). For smaller k , the Γ is related to $\text{Re}(\gamma)$, and it can be retyped as

$$\Gamma = k\gamma_1 + k^2\gamma_2 + \dots, \quad (45)$$

where γ_1 and γ_2 represent the first and second-order instability, respectively. After some lengthy computations,

$$\gamma_1 = \frac{8}{3} \left[\sqrt{\frac{8}{5} \cos^2 \theta - 1} + \imath \sin \theta \right], \quad (46)$$

the angle θ is in between the transverse component of the perturbation and the magnetic field. The first-order instability occurs when $\frac{8}{5}\cos^2\theta - 1 < 0$, that is, $\theta > 37.8^\circ$. Thus, the growth rate can be written as

$$\Gamma \simeq k\gamma_1 + O(k^2). \quad (47)$$

The second-order ($\sim k^2$) instability still occurs when $\theta < 37.8^\circ$ even if the configuration is stable for the first-order ($\sim k$) and, therefore, the growth rate reads as $\Gamma \simeq k^2\gamma_2 + O(k^3)$ [42], and the expression of γ_2 is given by

$$\gamma_2 = -\frac{4}{9} \left[\left(\frac{8}{5} \cos^2 \theta - 1 \right) \sec \theta + \frac{4(5 + 4 \cos^2 \theta) \tan \theta}{45 \sqrt{\frac{8}{5} \cos^2 \theta - 1}} \right]. \quad (48)$$

Allen and Rowlands' [42] instability analysis may be expressed in the following form.

When $\theta < \theta_{cr} \simeq 37.8^\circ$, then the instability growth rate can take the form

$$\Gamma = \Gamma_1 = k \operatorname{Re}(\gamma_1) + O(k^2) \simeq \frac{8}{3} k \sqrt{\frac{8}{5} \cos^2 \theta - 1}. \quad (49)$$

For $\theta > \theta_{cr} \simeq 37.8^\circ$, the instability growth rate reads

$$\Gamma = \Gamma_2 = k \operatorname{Re}(\gamma_2) + O(k^3) \simeq \frac{4}{9} k^2 (1 - 85 \cos^2 \theta) \sec \theta. \quad (50)$$

For transforming Equations (49) and (50) into our physical model, one needs to use the following transformation equations $\phi_0 = \frac{B}{AL_{\parallel}^2}$, $T_0 = \frac{L_{\parallel}^3}{B}$, $L_{\perp} = L_{\parallel} \left(\frac{C}{B} \right)^{1/2}$, respectively, for ϕ , time t , and (x, y) in order to transform Equation (43) into the planar ZK equation. Using the above transformation, we may use $k \rightarrow kL_{\perp}$, $\gamma_1 \rightarrow \gamma_1 T_0$, and $\gamma_2 \rightarrow \gamma_2 T_0$ in Equations (49) and (50), and finally we obtain the equations for growth rate instability as

$$\Gamma = \Gamma_1 \simeq \frac{8}{3} \frac{(BC)^{1/2}}{L_{\parallel}^2} k \sqrt{\frac{8}{5} \cos^2 \theta - 1}, \quad (51)$$

and

$$\Gamma = \Gamma_2 \simeq \frac{4C}{9L_{\parallel}} k^2 \left(1 - \frac{8}{5} \cos^2 \theta \right) \sec \theta. \quad (52)$$

The growth rate of the instability depends upon on varies plasma parameters, therefore it is important to study the effects of these parameters on the instability growth rate. The growth rate Γ_1 is plotted against θ for different plasma parameters as shown in Figure 6. It is clear that the growth rate goes to zero when $\theta \rightarrow \theta_{cr} \simeq 37.8^\circ$. Figure 6a indicates that for smaller values of θ ($0 \leq \theta < \theta_{cr}$), the growth rate Γ_1 increases as the nonextensivity q decreases. Figure 6b demonstrates the effect of parallel component of anisotropic ion pressure p_1 on the growth rate Γ_1 . It is shown that increasing p_1 leads to the reduction of the growth rate. The decreasing in perpendicular anisotropic ion pressure p_2 suppress the growth rate as depicted in Figure 6c. Figure 6d shows the effect of magnetic field strength Ω on growth rate Γ_1 which shows that growth rate is reduced with increasing Ω . Similarly, the second-order instability growth rate Γ_2 is plotted versus θ based on Equation (52) for different plasma parameters as shown in Figure 7. The figure clearly indicates that the growth rate increases sharply for $\theta > \theta_{cr}$. From Figure 7a, one can see that the growth rate Γ_2 grows with increasing the nonextensive parameter q and finally saturates at larger angles. The effect of parallel anisotropic ion pressure p_1 is shown in Figure 7b, the growth rate Γ_2 shrinks when p_1 is increased. Figure 7c illustrates the impact of anisotropic ion pressure p_2 on Γ_2 . It is seen that the increase of p_2 leads to a decrease in the growth rate Γ_2 . Figure 7d depicts the influence of the magnetic field strength Ω on growth rate Γ_2 , which we conclude that the growth rate Γ_2 is enhanced with increasing Ω .

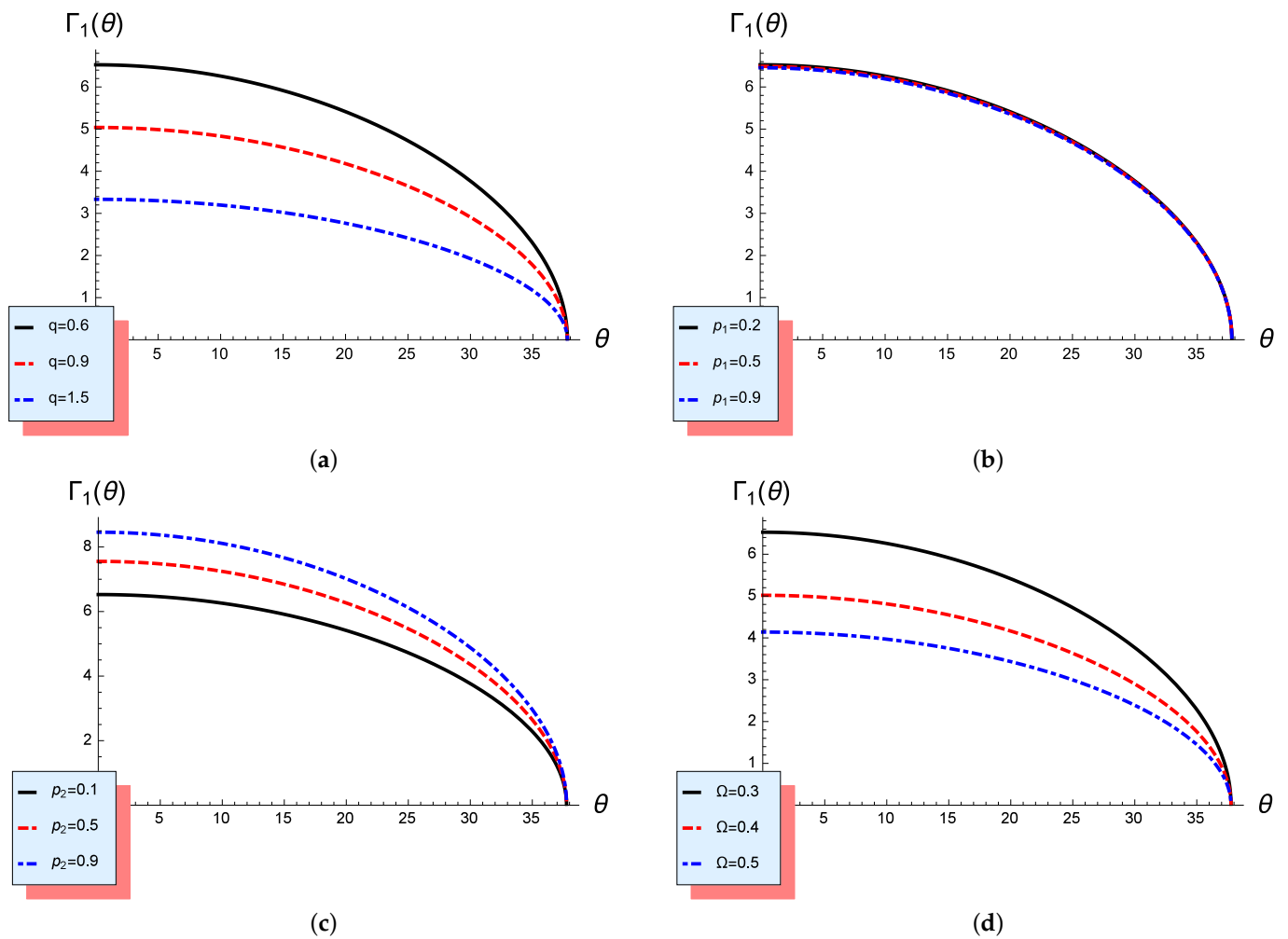


Figure 6. The first-order instability growth rate Γ_1 versus θ is plotted for fixed values of $ky = 0.05$, $L_{\parallel} = 0.2$ (a) for different values of q and $p_1 = 0.2$, $p_2 = 0.1$, $\Omega = 0.3$; (b) for different values of p_1 and $q = 0.6$, $p_2 = 0.1$, $\Omega = 0.3$; (c) for different values of p_2 and $q = 0.6$, $p_1 = 0.2$, $\Omega = 0.3$; and (d) for different values of Ω and $q = 0.6$, $p_1 = 0.2$, and $p_2 = 0.1$.

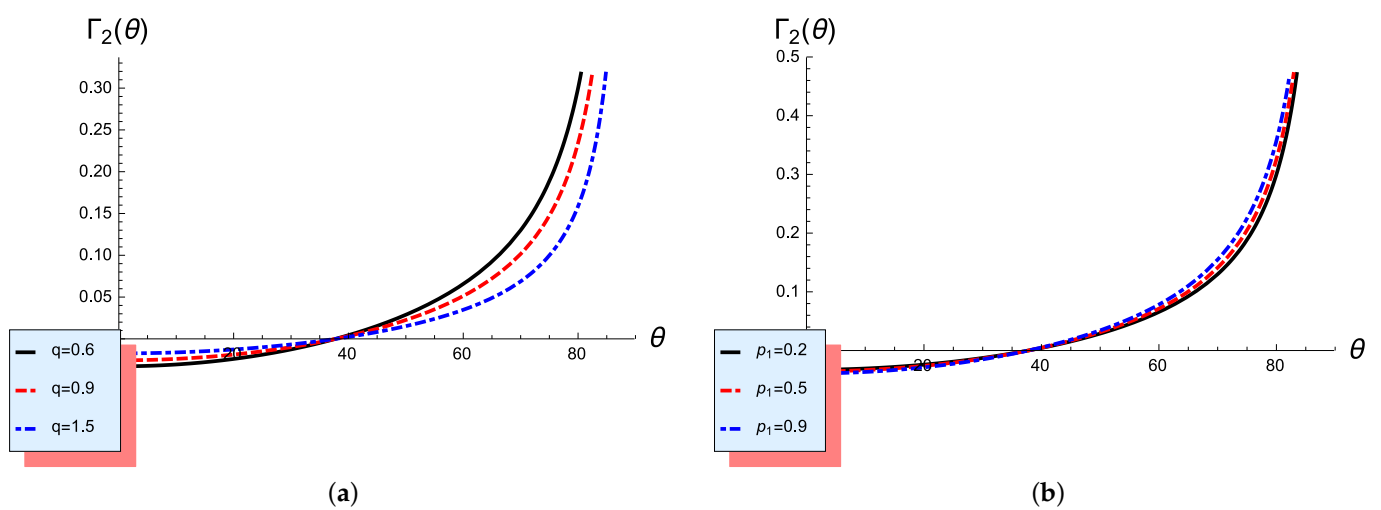


Figure 7. Cont.

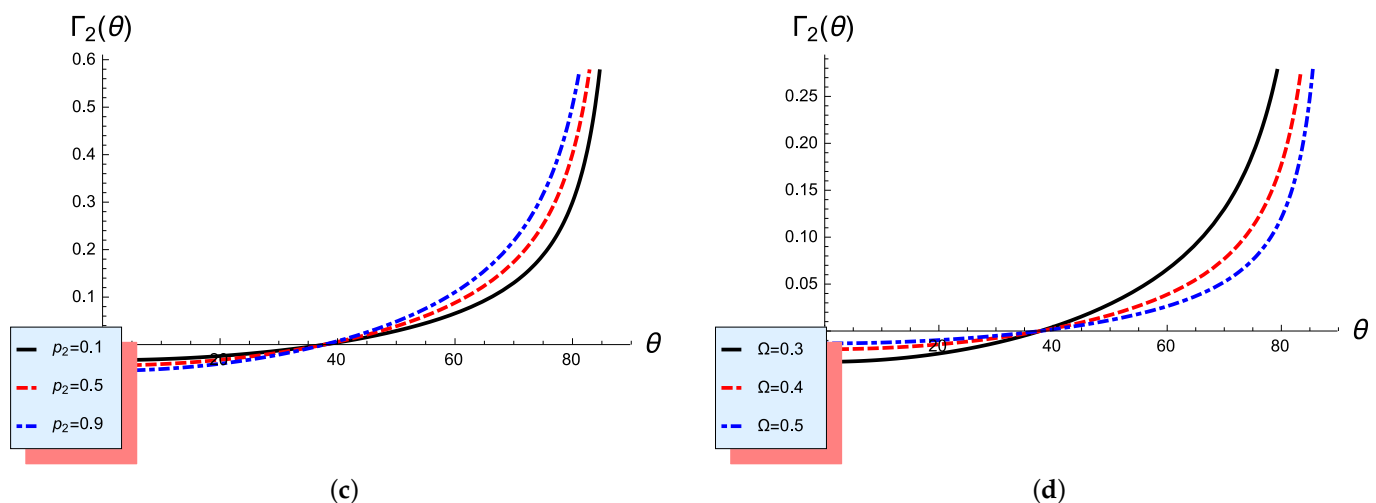


Figure 7. The second-order instability growth rate Γ_2 versus θ are plotted for fixed values of $ky = 0.05$, $L_{\parallel} = 0.2$ (a) for different values of q and $p_1 = 0.2$, $p_2 = 0.1$, $\Omega = 0.3$; (b) for different values of p_1 and $q = 0.6$, $p_2 = 0.1$, $\Omega = 0.3$; (c) for different values of p_2 and $q = 0.6$, $p_1 = 0.2$, $\Omega = 0.3$; and (d) for different values of Ω and $q = 0.6$, $p_1 = 0.2$, and $p_2 = 0.1$.

8. Conclusions

In the present article, the (non)linear ion-acoustic waves (IAWs) have been investigated in a magnetized plasma consists of warm ions and Tsalli distributed electrons. The effect of electron nonextensive parameter q , component of parallel anisotropic ion pressure p_1 , component of perpendicular anisotropic ion pressure p_2 and magnetic field strength Ω on both the linear and nonlinear IAWs has been studied. The main obtained results could be summarized as follows.

- The frequency of both slow and fast electrostatic modes decreases with increasing the electron nonextensivity parameter q . On the contrary, the frequency of both modes enhances with increasing the parallel anisotropic ion pressure p_1 . Moreover, the frequency of fast(slow) mode increases(decreases) with the enhancement of the perpendicular anisotropic ion pressure p_2 .
- The phase velocity of both slow and fast of the IAWs grows with Ω . Furthermore, the phase velocity decreases (increases) with the increasing the q (parallel anisotropic ion pressure p_1).
- The fluid equations of the present plasma model have been reduced to the ZK equation using the reductive perturbation technique. It was found that this model supports both the compressive and rarefactive nonlinear solitary structures.
- It was shown that the A increases while the B and C decrease with increasing the q . Increasing the p_1 significantly enhances the A and the C while the B shrinks. Furthermore, the dispersion coefficient C decreases when Ω increases.
- Both the amplitude and width of the ion-acoustic compressive soliton decay with increasing nonextensive parameter q and parallel anisotropic ion pressure p_1 . Increasing the perpendicular anisotropic ion pressure component p_2 leads the enhancement of the width of the ion-acoustic compressive solitary wave while amplitude remains unchanged.
- The approach of Allen and Rowlands was used for analyzing the solitary wave solution stability [42]. As a result, it was observed that raising the perpendicular anisotropic ion pressure p_2 enhances the growth rate Γ_1 , but increasing the nonextensive parameter q , parallel anisotropic ion pressure p_1 , and magnetic field Ω decreases the growth rate Γ_1 . Furthermore, increasing the nonextensivity q and magnetic field Ω increases the growth rate Γ_2 , but increasing the parallel anisotropic ion pressure p_1 and perpendicular anisotropic ion pressure p_2 suppresses the growth rate Γ_2 .

Finally, it is argued that the variables q , p_1 , p_2 , and Ω have a considerable impact on the features of the ion-acoustic nonlinear structures. Our findings might be useful in a wide variety of space observation and astrophysical scenarios where nonextensive electrons and pressure anisotropy are present [34,44–46].

Author Contributions: Conceptualization, M.K. and A.-u.-R.; methodology, M.K. and E.A.E.; software, M.K. and A.-u.-R.; validation, M.K., A.-u.-R. and E.A.E.; formal analysis, M.K., A.-u.-R. and S.A.E.-T.; investigation, M.K., A.-u.-R. and S.A.E.-T.; resources, M.K.; data curation, M.K.; writing—original draft preparation, A.A., S.K.E., S.A.A., E.A.E. and S.A.E.-T.; writing—review and editing, A.A., S.K.E., S.A.A., E.A.E. and S.A.E.-T.; visualization, M.K., A.-u.-R. and S.A.E.-T.; supervision, M.K., A.-u.-R. and S.A.E.-T.; project administration, A.A., S.K.E. and S.A.A.; funding acquisition, A.A. and S.K.E. All authors have read and agreed to the published version of the manuscript.

Funding: Supporting Project number (TURSP-2020/326), Taif University, Taif, Saudi Arabia.

Institutional Review Board Statement: Not applicable.

Informed Consent Statement: Not applicable.

Data Availability Statement: All data generated or analyzed during this study are included in this published article.

Acknowledgments: This work was supported by Taif University Researches Supporting Project number (TURSP-2020/326), Taif University, Taif, Saudi Arabia.

Conflicts of Interest: The authors declare no conflict of interest.

References

1. Tonks, L.; Langmuir, I. Oscillations in Ionized Gases. *Phys. Rev.* **1929**, *33*, 195.
2. Revans, R.W. The transmission of waves through an ionized gas. *Phys. Rev.* **1933**, *44*, 798. [\[CrossRef\]](#)
3. Walter, G.; Wise, J.; Pribyl, P.; Baker, R.; Layton, W.; Skrzypek, J.; Niknejadi, P.; Ransom, R.; Lee, D.; Zarinshenas, R.; et al. Ion acoustic wave experiments in a high school plasma physics laboratory. *Am. J. Phys.* **2007**, *75*, 103.
4. Saeed, R.; Mushtaq, A. Ion acoustic waves in pair-ion plasma: Linear and nonlinear analyses. *Phys. Plasmas* **2009**, *16*, 032307. [\[CrossRef\]](#)
5. Albalawi, W.; El-Tantawy, S.A.; Alkhateeb, S.A. The phase shift analysis of the colliding dissipative KdV solitons. *J. Ocean Eng. Sci.* **2021**, in press. [\[CrossRef\]](#)
6. El-Tantawy, S.A.; Salas, A.H.; Alharthi, M.R. On the dissipative extended Kawahara solitons and cnoidal waves in a collisional plasma: Novel analytical and numerical solutions. *Phys. Fluids* **2021**, *33*, 106101. [\[CrossRef\]](#)
7. Aljahdaly, N.H.; El-Tantawy, S.A. Simulation study on nonlinear structures in nonlinear dispersive media. *Chaos Interdiscip. Nonlinear Sci.* **2020**, *30*, 053117. [\[CrossRef\]](#)
8. Khalid, M.; El-Tantawy, S.A. Oblique ion acoustic excitations in a magnetoplasma having k -deformed Kaniadakis distributed electrons. *Astrophys. Space Sci.* **2020**, *365*, 75. [\[CrossRef\]](#)
9. Kashkari, B.S.; El-Tantawy, S.A.; Salas, A.H.; El-Sherif, L.S. Homotopy perturbation method for studying dissipative nonplanar solitons in an electronegative complex plasma. *Chaos Solitons Fractals* **2020**, *130*, 109457. [\[CrossRef\]](#)
10. Albalawi, W.; El-Tantawy, S.A.; Salas, A.H. On the rogue wave solution in the framework of a Korteweg–de Vries equation. *Results Phys.* **2021**, *30*, 104847. [\[CrossRef\]](#)
11. Washimi, H.; Taniuti, T. Propagation of ion-acoustic solitary waves of small amplitude. *Phys. Rev. Lett.* **1966**, *17*, 996. [\[CrossRef\]](#)
12. Sagdeev, R.Z. Cooperative phenomena and shock waves in collisionless plasmas. *Rev. Plasma Phys.* **1966**, *4*, 23.
13. Ikezi, H.; Taylor, R.; Baker, D. Formation and interaction of ion-acoustic solitons. *Phys. Rev. Lett.* **1970**, *25*, 11. [\[CrossRef\]](#)
14. Saini, N.S.; Shalini. Ion acoustic solitons in a nonextensive plasma with multi-temperature electrons. *Astrophys. Space Sci.* **2013**, *346*, 155. [\[CrossRef\]](#)
15. Renyi, A. On a new axiomatic theory of probability. *Acta Math. Hung.* **1955**, *6*, 285. [\[CrossRef\]](#)
16. Tsallis, C. Possible generalization of Boltzmann–Gibbs statistics. *J. Stat. Phys.* **1988**, *52*, 479. [\[CrossRef\]](#)
17. Lima, J.A.S.; Silva, R.J.; Santos, J. Plasma oscillations and nonextensive statistics. *Phys. Rev. E* **2000**, *61*, 3260.
18. Du, J. Nonextensivity in nonequilibrium plasma systems with Coulombian long-range interactions. *Phys. Lett. A* **2004**, *329*, 262. [\[CrossRef\]](#)
19. Liyan, L.; Du, J. Ion acoustic waves in the plasma with the power-law q -distribution in nonextensive statistics. *Phys. A* **2008**, *387*, 4821. [\[CrossRef\]](#)
20. Amour, R.; Tribeche, M. Variable charge dust acoustic solitary waves in a dusty plasma with a -nonextensive electron velocity distribution. *Phys. Plasmas* **2010**, *17*, 063702. [\[CrossRef\]](#)

21. Livadiotis, G. Approach on Tsallis statistical interpretation of hydrogen-atom by adopting the generalized radial distribution function. *J. Math. Chem.* **2009**, *45*, 930. [\[CrossRef\]](#)
22. Hanel, R.; Thurner, S. Stability criteria for q-expectation values. *Phys. Lett. A* **2009**, *373*, 1415. [\[CrossRef\]](#)
23. Pakzad, H.R. Effect of q-nonextensive electrons on electron acoustic solitons. *Phys. Scr.* **2011**, *83*, 015505. [\[CrossRef\]](#)
24. Tribeche, M.; Merriche, A. Nonextensive dust-acoustic solitary waves. *Phys. Plasmas* **2011**, *18*, 034502. [\[CrossRef\]](#)
25. Ghosh, U.N.; Chatterjee, P.; Kundu, S.K. The effect of q-distributed ions during the head-on collision of dust acoustic solitary waves. *Astrophys. Space Sci.* **2012**, *339*, 255. [\[CrossRef\]](#)
26. Cairns, R.A.; Mamun, A.A.; Bingham, R.; Shukla, P.K. Ion-acoustic solitons in a magnetized plasma with nonthermal electron. *Phys. Scr.* **1996**, *T63*, 80. [\[CrossRef\]](#)
27. Mamun, A.A.; Cairns, R.A. Stability of solitary waves in a magnetized non-thermal plasma. *J. Plasma Phys.* **1996**, *56*, 175. [\[CrossRef\]](#)
28. Zakharov, V.E.; Kuznetsov, E.A. Three-dimensional solitons. *Zh. Eksp. Teor. Fiz.* **1974**, *66*, 594.
29. Laedke, E.W.; Spatschek, K.H. Growth rates of bending KdV solitons. *J. Plasma Phys.* **1982**, *28*, 469. [\[CrossRef\]](#)
30. Infeld, E. Self-focusing of nonlinear ion-acoustic waves and solitons in magnetized plasmas. *J. Plasma Phys.* **1985**, *33*, 171. [\[CrossRef\]](#)
31. Das, K.P.; Verheest, F. Ion-acoustic solitons in magnetized multi-component plasmas including negative ions. *J. Plasma Phys.* **1989**, *41*, 139. [\[CrossRef\]](#)
32. El-Taibany, W.F.; El-Bedwehy, N.A.; El-Shamy, E.F. Three-dimensional stability of dust-ion acoustic solitary waves in a magnetized multicomponent dusty plasma with negative ions. *Phys. Plasmas* **2011**, *18*, 033703. [\[CrossRef\]](#)
33. Chew, G.F.; Goldberger, M.L.; Low, F.E. The Boltzmann equation and the one-fluid hydromagnetic equations in the absence of particle collisions. *Proc. R. Soc. Lond.* **1956**, *A236*, 112.
34. Denton, R.E.; Anderson, B.J.; Gary, S.P.; Fuselier, S.A. Bounded anisotropy fluid model for ion temperatures. *J. Geophys. Res.* **1994**, *99*, 11. [\[CrossRef\]](#)
35. Khalid, M.; Rahman, A.-u. Ion acoustic cnoidal waves in a magnetized plasma in the presence of ion pressure anisotropy. *Astrophys. Space Sci.* **2019**, *364*, 28. [\[CrossRef\]](#)
36. Khalid, M.; Hadi, F.; Rahman, A. Ion-scale cnoidal waves in a magnetized anisotropic superthermal plasma. *J. Phys. Soc. Jpn.* **2019**, *88*, 114501. [\[CrossRef\]](#)
37. Silva, R., Jr.; Plastino, A.; Lima, J. A Maxwellian path to the q-nonextensive velocity distribution function. *Phys. Lett. A* **1998**, *249*, 401. [\[CrossRef\]](#)
38. Verheest, F. Ambiguities in the Tsallis description of non-thermal plasma species. *J. Plasma Phys.* **2013**, *79*, 1031–1034. [\[CrossRef\]](#)
39. El-Tantawy, S.A. Effect of ion viscosity on dust ion-acoustic shock waves in a nonextensive magnetoplasma. *Astrophys. Space Sci.* **2016**, *361*, 249. [\[CrossRef\]](#)
40. El-Tantawy, S.A.; Wazwaz, A.-M.; Schlickeiser, R. Solitons collision and freak waves in a plasma with Cairns-Tsallis particle distributions. *Plasma Phys. Control.* **2015**, *57*, 125012. [\[CrossRef\]](#)
41. El-Tantawy, S.A.; El-Bedwehy, N.A.; Moslem, W.M. Super rogue waves in ultracold neutral nonextensive plasmas. *J. Plasma Phys.* **2013**, *79*, 1049. [\[CrossRef\]](#)
42. Allen, M.A.; Rowlands, G. Stability of obliquely propagating plane solitons of the Zakharov-Kuznetsov equation. *J. Plasma Phys.* **1995**, *53*, 63. [\[CrossRef\]](#)
43. Adnan, M.; Williams, G.; Qamar, A.; Mahmood, S.; Kourakis, I. Pressure anisotropy effects on nonlinear electrostatic excitations in magnetized electron-positron-ion plasmas. *Eur. Phys. J. D* **2014**, *68*, 247. [\[CrossRef\]](#)
44. Barkan, A.; D'Angelo, N.; Merlino, R.L. Experiments on ion-acoustic waves in dusty plasmas. *Planet. Space Sci.* **1996**, *44*, 239. [\[CrossRef\]](#)
45. Baumjohann, W.; Treumann, R.A. *Basic Space Plasma Physics*; Imperial College Press: London, UK, 1997.
46. Nakamura, Y.; Sharma, A. Observation of Ion-Acoustic Solitary Waves in a Dusty Plasma. *Phys. Plasmas* **2001**, *8*, 3921. [\[CrossRef\]](#)